Materials Science and Engineering A366 (2004) 183–194

MATERIALS SCIENCE & ENGINEERING A

www.elsevier.com/locate/msea

Thixocasting of hypereutectic Al–25Si–2.5Cu–1Mg–0.5Mn alloys using densified powder compacts

C.M. Chen [a,b,*], C.C. Yang [b], C.G. Chao [a]

[a] *Institute of Materials Science and Engineering, National Chiao Tung University, Hsingchu, Taiwan 310, ROC*
[b] *Materials Research Laboratories, Industrial Technology Research Institute, J100, Bldg 77, 195-5 Chung Hsing Rd., Section 4, Chutung, Hsinchu, Taiwan 310, ROC*

Received 15 May 2003; received in revised form 10 September 2003

Abstract

Hypereutectic Al–Si alloys with fine and evenly distributed Si grains have superior mechanical characteristics and are usually fabricated by powder metallurgy (PM). However, PM methods cannot easily achieve the net-shape forming of complicated engineering parts. This work presents a novel method, which combines consolidating prealloyed powders with thixocasting the consolidated compacts, for net-shape forming of a hypereutectic Al–25Si–2.5Cu–1Mg–0.5Mn alloy. Experimental results indicate that as-thixocast specimens fabricated with larger powders and greater deformations have higher tensile strengths. Fractographs show that the strengths were strongly affected by the detrimental oxides that originated in the powder compacts, and that the oxides could be effectively eliminated by plastic deformation during thixocasting. Isothermal heat-treatment tests of the powders revealed two distinct ranges of Si grain-coarsening rates in the semi-solid temperature range. The Si grains ripened slowly at temperatures from 540 to 560 °C, considered as the appropriate processing temperature range for obtaining fine Si grain. This low coarsening rate was explained by the diffusion of Si through the semi-solid matrix that only consists of a little liquid, since Si diffuses in solid Al much more slowly then in liquid Al.

Keywords: Hypereutectic Al–Si alloys; Semi-solid; Thixocast; Powder consolidation

1. Introduction

Hypereutectic Al–Si–X alloys have good wear resistance, high stiffness, and low thermal expansion. They are extensively used for making light-weight wearing parts such as engine pistons, cylinder liners, compressor scrolls and engine blocks [1,2]. These parts are traditionally produced by casting or powder metallurgy (PM). In castings, however, coarse Si grains are present even though modifying treatments are used [1,2]. Additionally, since the Si grains are slightly lighter than the melt and tend to float, castings that solidify slowly can exhibit pronounced gravitational segregation of Si particles [1]. These segregated large Si grains may shorten the life of the tools used in machining and also dramatically degrade the mechanical properties [3]. As for PM methods, they are well known processes for fabricating hypereutectic Al–Si–X alloys with fine Si grains. Nevertheless, sintering aluminum alloy powder is difficult because of the presence of surface oxides. During the last two decades, techniques for powder forging [3] or powder extrusion [4,5] have been developed to overcome this difficulty. These methods have been successfully applied to producing compressor scrolls [3] and bulk materials of hypereutectic Al–Si–X alloy [4,5]. However, these proposed techniques still cannot easily achieve net-shape forming of several engineering parts, such as engine pistons, because the powder compacts in the solid state exhibit limited formability. A backpressure is often required in conventional powder forging machines, complicating the design of the forging molds and the machines, hence increasing costs [6].

Since the discovery of the unique rheological behavior of nondendritic semi-solid slurries in the early 1970s [7,8], several new semi-solid metal-forming (SSMF) processes based on nondendritic semi-solid slurries have been developed. Thixocasting [9] is an SSMF process in which the net-shape forming of specimens is performed by die-casting metal slurries heated from a solid state to a semi-solid state. Normally, the nondendritic feedstock used for thixocasting is made

* Corresponding author. Tel.: +886-3-591-6987; fax: +886-3-582-0207.
E-mail address: mu@itri.org.tw (C.M. Chen).

0921-5093/$ – see front matter © 2003 Elsevier B.V. All rights reserved.
doi:10.1016/j.msea.2003.09.063

by an ingot casting method. The most popular feedstock used for thixocasting is currently hypereutectic Al–Si alloy, and is mostly produced by continuous casting with electromagnetic stirring of the melt during solidification. However, ingot casting of hypereutectic Al–Si alloys with fine microstructures is difficult, as the solidification during cooling is so slow that the coarsening of Si grains may readily occur. A method for fabricating the hypereutectic Al–Si–Cu feedstock for thixocasting was recently developed using a combination of spray forming and extrusion [10]. An Al-25Si-5Cu oil pump housing has been shown to be successfully thixocast using this feedstock [10]. However, this procedure also has many drawbacks, including the low yield of spray forming of around 60–80% due to over spraying [10], and increased costs due to a greater investment in spray forming equipment.

The aim of this study is to evaluate the new method of thixocasting hypereutectic Al–25Si–2.5Cu–1Mg–0.5Mn alloys using feedstock made by the traditional powder consolidation method. This new method of thixocasting hypereutectic Al–Si alloys is introduced as the powder-thixocasting process in the following paragraphs. The effects of processing parameters on the microstructure and tensile strength of thixocast specimens were examined. Results show that this novel method is preferentially suitable for net-shape forming of hypereutectic alloys with fine microstructures.

2. Experimental

2.1. Materials

The hypereutectic powders used were supplied by Valimet Inc USA, and have nominal compositions of Al–25Si–2.5Cu–1Mg–0.5Mn (in weight percent), and their chemical compositions are given in Table 1. The as-atomized powders were sieved and divided into three groups with different particle size ranges, namely fine (<45 μm), medium (45–120 μm) and coarse (120–300 μm). Particle size distributions of the three fractions of the Al–Si powders were measured by a particle size analyzer, Beckman Coulter™. The values of particle size are listed in Table 2, where d_{10}, d_{50} and d_{90} present the particle diameters such that 10, 50 and 90%, respectively, of the total powder volume is in particles of smaller diameter.

Table 1
Chemical compositions of the hypereutectic Al–25Si–2.5Cu–1Mg–0.5Mn alloy powder

Element	Rate (wt.%)
Si	24.64
Cu	2.56
Mg	1.04
Mn	0.47
Fe	0.16
Ni	0.01
Ti	0.03
Al	Bal.

Table 2
Particle size distributions of the three fractions of the gas atomized Al–Si powder

Fraction (μm)	Powder size (μm)		
	d_{10}	d_{50}	d_{90}
<45	14	32	42
45–120	50	78	114
120–300	135	175	240

2.2. Properties of materials

The powders were characterized by the following two tests to determine adequate processing temperatures for thixocasting.

2.2.1. Differential thermal analysis

The range of temperature, where the melting and solidification of the powders occurs, was revealed by differential thermal analysis (DTA), using a Du Pont Thermal Analyst 2100. In DTA tests, 40 mg powder was charged in an alumina crucible, heated at a rate of 10 °C/min to 800 °C and then cooled at 10 °C/min.

2.2.2. Isothermal heat-treatment tests

The growth behavior of Si grains in the hypereutectic powders was revealed by isothermal heat-treatment tests. In each test, approximately 1 g of powder was heated in a crucible in an electric furnace. The Si grain sizes were measured by the method of linear intercept. The mean linear intercepts L were the average of the linear intercepts of at least 100 Si grains measured for atomized powders with different areas, obtained using an optical microscope. The polyhedral Si grains were assumed to be uniform spheres, whose diameters d were calculated according to the relationship $d = 3L/2$, to simplify the calculation.

2.3. Powder-thixocasting

A novel process, combining powder densification and thixocasting, has been recently developed and presented elsewhere, for the net-shape forming of hypereutectic Al–Si–X alloys [12]. Fig. 1a–d schematically depicts the processing procedures. In this work, approximately 1 kg of the hypereutectic Al–25Si–2.5Cu–1Mg–0.5Mn prealloyed powders were first preheated to 500 or 550 °C in an argon atmosphere in an electric furnace, as depicted in Fig. 1a. Then, the preheated powder was consolidated using an uniaxial hydraulic press at a pressure of 85 MPa to form green powder compacts with a diameter of 76 mm, as shown in Fig. 1b. Then, the consolidated compacts were quickly heated into a semi-solid state using an induction coil, as depicted in Fig. 1c. The compacts were heated to 555–560 °C

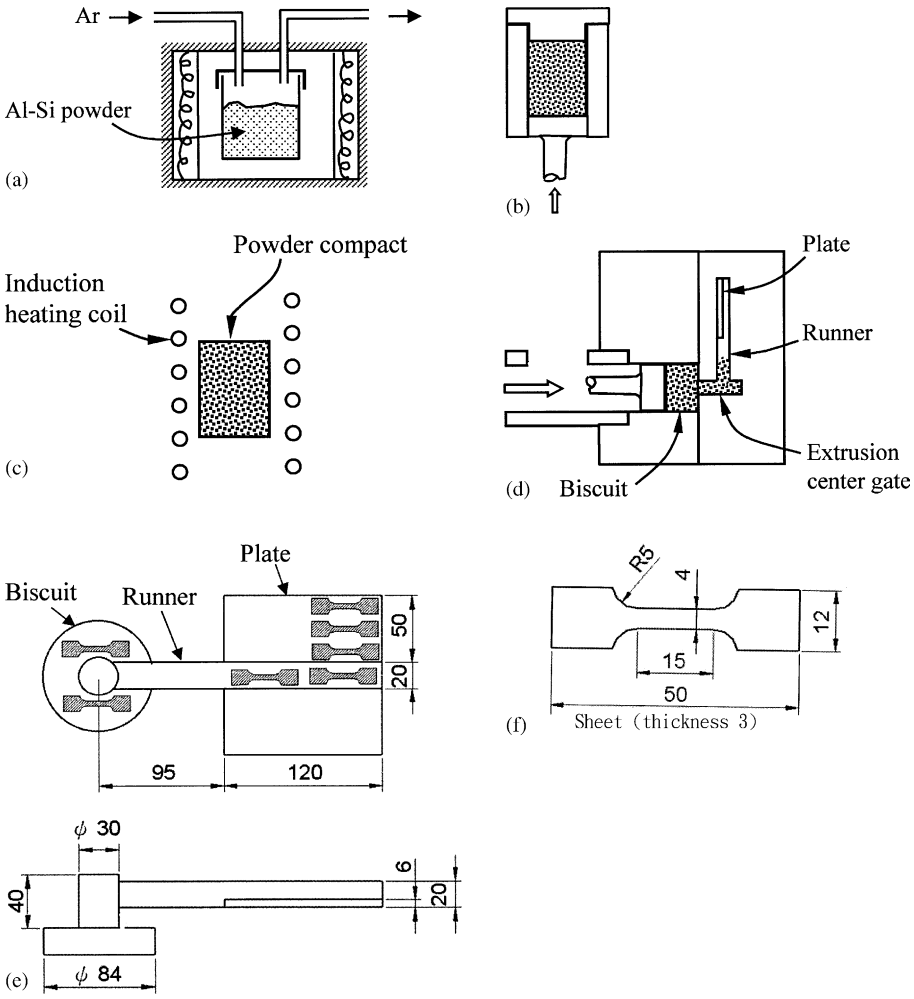

Fig. 1. Schematic diagram of the powder-thixocasting process: (a) preheating the hypereutectic prealloyed Al–Si powders, (b) hot consolidating the powders into compacts, (c) heating the compacts into a semi-solid state with induction coils, and (d) thixocasting the semi-solid compacts by a high-pressure die-casting machine. The location of the three different sections is schematically shown in (d). The dimensions of the thixocast and tensile specimens are shown in (e) and (f), respectively.

in 200 s to prevent excess oxidation. The heated semi-solid compacts were immediately transported into the sleeve of a high-pressure die-casting machine and then injected into a mold cavity at a plunger pressure of 90 MPa and a plunger velocity of 1 m/s, as shown in Fig. 1d. The thixocast specimen is divided into three zones "biscuit, runner, plate", which are schematically shown in Fig. 1d. During thixocasting, a plunger squeezed the semi-solid powder compact in a sleeve—the zone of "biscuit". Afterwards, the powder compact was extruded and flew through the center gate and the "runner" to reach the zone of "plate". Fig. 1e shows the dimensions of the thixocast specimen.

2.4. Properties of the powder-thixocast specimens

2.4.1. Thermal treatment-T6

Since the Al–Si hypereutectic alloys used are heat treatable, a thermal treatment-T6 was applied to the as-thixocast specimens to investigate their peak strength. The T6-treated specimens were heated at 500 °C for 4 h and then heated at 175 °C for 10 h.

2.4.2. Density and tensile properties

Density test specimens of 5 mm × 5 mm × 5 mm and tensile test specimens were machined from three sections of the thixocast specimens, as shown in Fig. 1e. Densities were measured by applying Archimedes' Principle. Dimensions of tensile test specimens are shown in Fig. 1f. Tensile tests were conducted using an Instron 4469 machine at a crosshead speed of 1.7×10^{-5} m/s. Each tensile and density value was an average obtained from three specimens.

2.4.3. Fractographs and microstructures

The tensile fracture surfaces were examined using a Cambridge S-360 Scanning electron microscope (SEM). The microstructures of the powders and thixocast specimens etched with a 0.5% HF water solution were examined using an optical microscope.

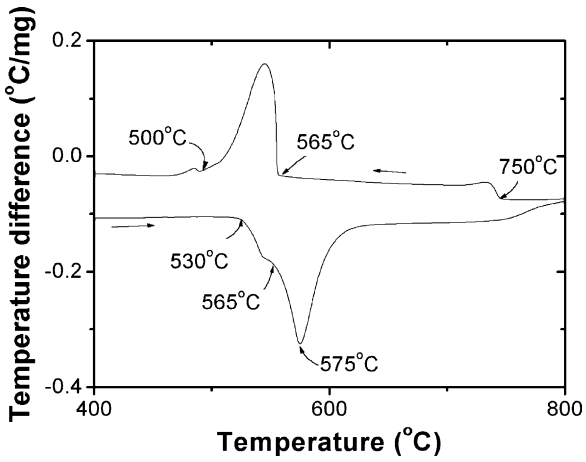

Fig. 2. Differential thermal analysis (DTA) scan of the hypereutectic Al–25Si–2.5Cu–1Mg–0.5Mn powders in size of 120–300 μm.

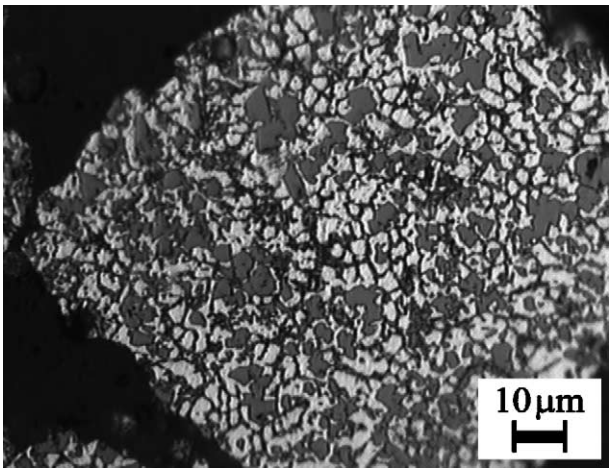

Fig. 3. Optical microstructures of the as-atomized hypereutectic Al–25Si–2.5Cu–1Mg–0.5Mn powders in size of 120–300 μm.

3. Results

3.1. Characteristics of the powders

3.1.1. Range of temperatures of solidification

The three groups of the used powders—fine (<45 μm), medium (45–120 μm) and coarse (120–300 μm), have DTA curves with almost the same features, even though the smaller powders have finer microstructures. Fig. 2 plots a typical DTA curve, showing that the range of temperatures over which solidification occurs is from about 750–500 °C. Upon heating, two endothermic peaks appear at on-set temperatures of 530 and 565 °C. Three exothermic peaks exhibited during cooling, at the on-set temperatures of 750, 565 and 500 °C.

3.1.2. Isothermal Si grain growth

Fig. 3 shows an optical micrograph of the as-atomized hypereutectic Al–25Si–2.5Cu–1Mg–0.5Mn powder. Fig. 4a–c present optical micrographs of the powders isothermally heat-treated at 500, 550 and 600 °C for 1 h, respectively. Comparing Figs. 3 and 4 shows that the Si grains did not clearly become coarser after they were isothermally heat-treated at 500 and 550 °C; but they did apparently become coarser after isothermal heat-treatment at 600 °C for 1 h. A series of isothermal heat-treatment tests were performed to clarify this Si grain-coarsening behavior. Table 3 lists the results, which clearly show that the size of the Si grains increased with the heat-treatment temperature and period.

It is noted in Fig. 3 that there is a black "network" in the Al-grains of the as-atomized powder. However, this network is not visible in the heat-treated powders (Fig. 4). The microconstituents of the black "network" (Fig. 3) would contain the eutectic phases of α-Al and Si, which generally exhibit in the chill-cast hypereutectic Al–Si alloy [1], along with other phases such as Mg_2Si, Al_2Cu, $Al_{15}(Mn,Fe)_3Si_2$, $Al_5Mg_8Cu_2Si_6$ etc [13,14]. After heat-treating at 500 or 600 °C, some of these phases dissolved into the α-Al matrix according to the solubility of the element in α-Al. The phases that did not dissolve completely, such as eutectic Si and Al_2Cu, would grow up during heat-treating. This coarsening would yield several small particles distributed around the primary Si as shown in Fig. 4.

3.2. Characteristics of the powder compacts

Fig. 5a–c shows a series of optical micrographs with representative microstructures of the green compacts consolidated at various temperatures. Comparing Fig. 5a and b reveal that the compacts consolidated at 500 °C had much more inter-granular pores than those consolidated at 550 °C. According to the DTA results, the powders are in a solid state at 500 °C and in a semi-solid state at 550 °C. Thus Fig. 5a and b revealed clearly that the powders in the semi-solid

Table 3
The particle sizes (μm) variations of Si grains in the coarse powders (120–300 μm) with isothermal heat-treatment temperatures and time intervals

Time (h)	Isothermal heat-treatment temperature (°C)						
	500	540	550	560	570	580	600
1	7.5 ± 2.5	9.9 ± 4.8	10.8 ± 8.4	11.0 ± 4.0	17.2 ± 11.7	18.9 ± 5.7	22.8 ± 9.9
2	8.7 ± 2.7	10.8 ± 5.6	12.4 ± 5.1	13.4 ± 5.4	21.6 ± 8.9	24.6 ± 14.1	28.5 ± 10.7
4	8.8 ± 2.8	12.8 ± 7.9	13.3 ± 6.5	15.9 ± 7.2	27.7 ± 11.4	31.5 ± 18.1	35.5 ± 11.9

The Si particle size in the as-atomized powder is 8.1 ± 2.7 μm.

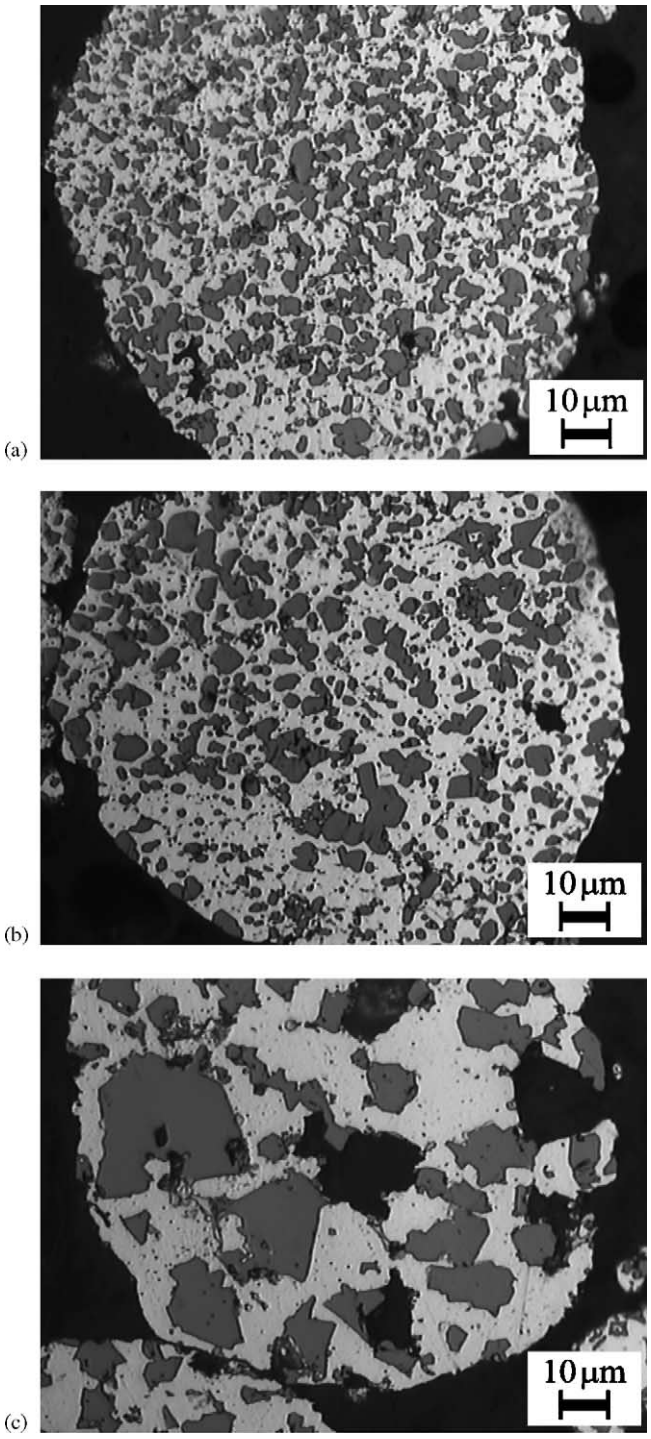

Fig. 4. Optical microstructures of the as-atomized hypereutectic Al–25Si–2.5Cu–1Mg–0.5Mn powders in size of 120–300 μm after isothermal heat-treatment at (a) 500 °C, (b) 550 °C, and (c) 600 °C, for 1 h.

state were much more compressible than those in the fully solid state. Fig. 5c presents the micrograph of the powder compact consolidated at 600 °C, and shows that some liquid was squeezed out of the powders, filling the inter-granular pores of the compacts. In this case, although the density of the compacts became very high, the Si grains became

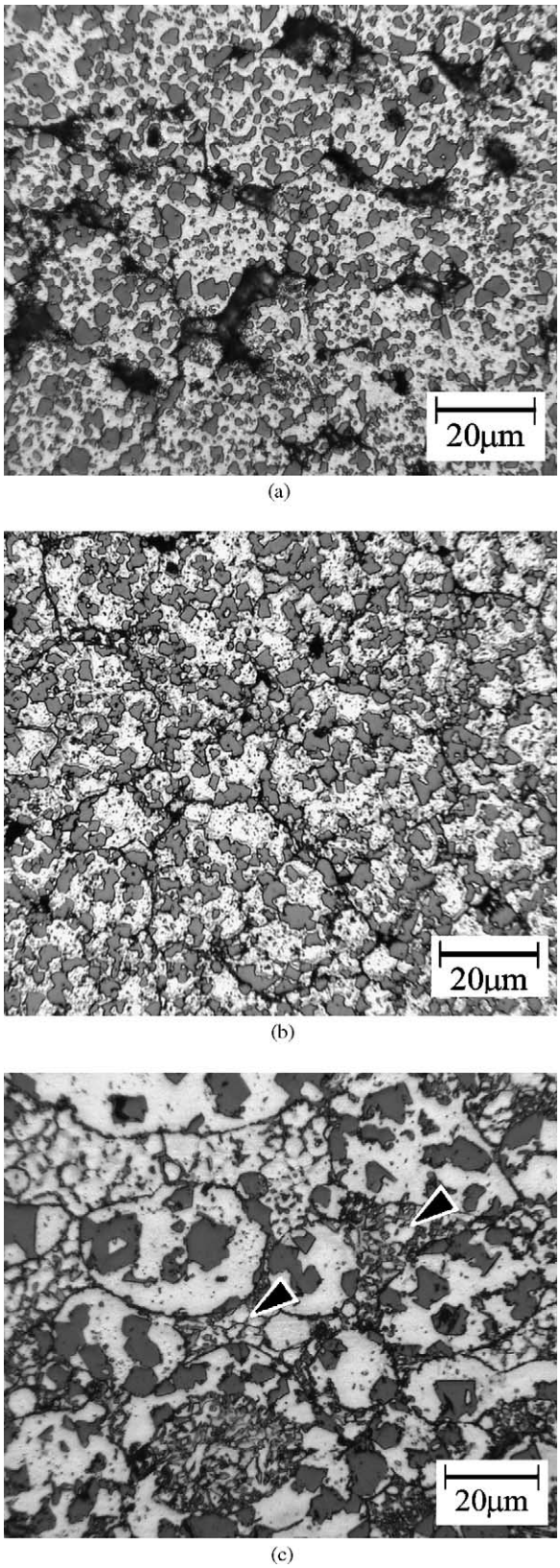

Fig. 5. Optical microstructures of the green powder compacts consolidated at (a) 500 °C, (b) 550 °C, and (c) 600 °C with the hypereutectic Al–25Si–2.5Cu–1Mg–0.5Mn powders in size of <45 μm; the arrows indicate the region where the melt was squeezed out of the powder.

Table 4
The relative densities (%) of the green powder compacts consolidated at different temperatures and with different sizes of powders

Powder size	Powder consolidation temperature (°C)				
	250	400	500	550	600
<45 μm	–	–	79	93	97
45–120 μm	60	67	75	92	96
120–300 μm	–	–	74	90	95

much coarser. This severe Si grain growth was consistent with the results of the isothermal heat-treatment tests of the powder.

Table 4 lists the relative density of the powder compacts as a function of powder size and powder consolidation temperature. The relative density is the ratio of the compact density to the theoretical density of the bulk materials. Table 4 shows that the relative density increased quickly with the consolidating temperature, but fell slightly as the size of the powder increased. The compacts consolidated at 250 and 400 °C had relative densities that were too low, such that they were too weak to be handled. However, the compacts consolidated at 600 °C showed the detrimental effect of Si grain growth. Consequently, only two powder consolidating temperatures, 500 and 550 °C, were used for thixocasting herein. The effects of the two consolidating temperatures on the thixocast specimen are considered below.

3.3. Microstructures and densities of powder-thixocast specimens

Fig. 6 is the typical microstructure of a powder-thixocast specimen, showing fine and evenly distributed Si grains, with a mean size of only around 15 μm. Unlike in Fig. 5a and b, Fig. 6 shows that both oxide layers on the powder interfaces and the inter-granular pores almost vanished after thixocasting, implying that the new powder-thixocasting process presented herein can effectively consolidate the Al–Si powders. The extent of the elimination of inter-granular pores can also be related to the relative density of a thixocast specimen, as shown in Table 5. The table shows that the relative densities of thixocast specimens are much higher than those of green powder compacts, shown in Table 4, indicating that most of the inter-granular pores in the powder compacts were eliminated after thixocasting.

Table 5
The densities and relative densities of the Al–25Si–2.5Cu–1Mg–0.5Mn thixocast specimens in different positions depicted in Fig. 1e

Specimen position	Consolidating temperatures					
	500 °C			550 °C		
	Biscuit	Runner	Plate	Biscuit	Runner	Plate
Density	2.558	2.556	2.606	2.596	2.569	2.609
Relative density (%)	96.5	96.4	98.2	97.9	96.8	98.4

The specimens were thixocast using the feedstock of powder compacts consolidated at different temperatures.

3.4. Strengths of powder-thixocast specimens

Table 6 lists the ultimate tensile strengths of the powder-thixocast specimens measured from different sections of the thixocast specimens, as depicted in Fig. 1e. Notably, the tensile strengths varied greatly from section to section of the powder-thixocast specimens. The specimens were strongest in the "plate" section and weakest in the "biscuit" section. For example, for the thixocast specimens fabricated from powders of fine size (<45 μm) and compacts consolidated at 550 °C, the strength of the "runner" (129.7 MPa) and the "plate" (210.3 MPa) were increased by 62 and 120%, respectively, over that of the "biscuit" (95.7 MPa). Table 6 also

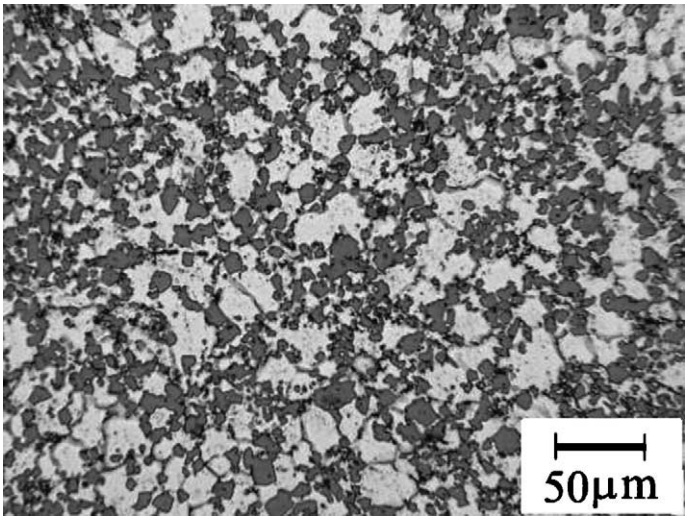

Fig. 6. Optical microstructure of the hypereutectic Al–25Si–2.5Cu–1Mg–0.5Mn powder-thixocast specimen obtained from "plate" section as depicted in Fig. 1e. The specimen was thixocast using compacts consolidated at 550 °C and powders in size of 120–300 μm.

Table 6
Ultimate tensile strengths (MPa) of the Al–25Si–2.5Cu–1Mg–0.5Mn thixocast specimens in different positions depicted in Fig. 1e and using the powder compacts consolidated at different temperatures

Powder size (μm)	Consolidating temperatures					
	500 °C			550 °C		
	Biscuit	Runner	Plate	Biscuit	Runner	Plate
<45	[a]	89.6 ± 11.9	178.0 ± 10.7	95.7 ± 59.2	129.7 ± 32.0	210.3 ± 13.4
45–120	[a]	128.6 ± 17.8	163.4 ± 28.0	152.1 ± 53.6	184.4 ± 20.4	210.7 ± 5.0
120–300	–	–	193.2 ± 25.2	–	–	224.7 ± 4.5 (304 ± 6.5)

[a] Materials are so brittle that tensile specimen cannot be machined.

shows that the powder-thixocast specimens fabricated from smaller powders exhibited a slightly lower tensile strength. The thixocast specimens fabricated using the powder compacts consolidated at 550 °C clearly had a higher tensile strength than those fabricated using compacts consolidated at 500 °C.

In Table 6, the specimens that have the optimum strength are those fabricated using consolidation temperature at 550 °C, powder size in 120–300 μm, and zone of "plate". The stress–strain curves of this specimen in as-thixocast and T6 state are shown in Fig. 7, indicating brittle behavior of this specimen. In this study if the as-thixocast specimens in Table 5 had strength value below 150 MPa, the maximum strength in elastic deformation regime as shown in Fig. 7, they almost fractured in elastic deformation zone during tensile tests and exhibited little plastic fracture strain.

3.5. Fractographs

Figs. 8 and 9 show representative tensile fractographs of the thixocast specimens fabricated using powder compacts consolidated at 500 and 550 °C, respectively. In Fig. 8, the fracture surfaces exhibit many dimples and cleavage planes. However, besides these dimples and cleavages, several deep

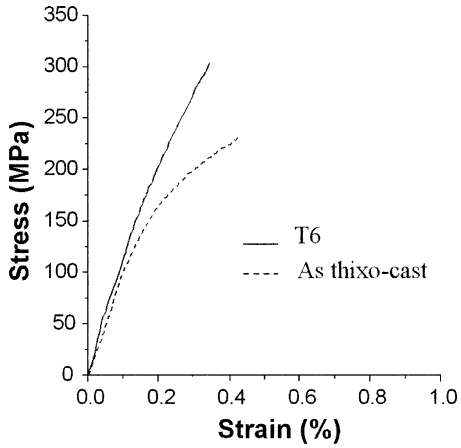

Fig. 7. Stress–strain curves of the tensile specimen machined from the "plate" sections of the thixocast specimen fabricated using powders of size in 120–300 μm and compacts consolidated at 550 °C.

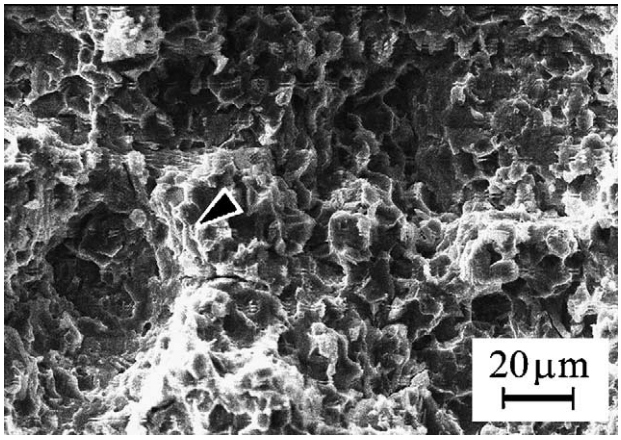

Fig. 8. Tensile fractograph of the powder-thixocast specimens fabricated using powders in size of 45–120 μm and compacts consolidated at 500 °C. (▽) Indicates spherical caves caused by powder decohesion.

spherical caves also can be noted in the Fig. 8. These spherical caves were considered to be formed by the decohesion of the powders at the interface, resulting from incomplete elimination of the detrimental oxide film on the powders after thixocasting. However, the deep spherical caves have not been found in the thixocast specimens fabricated using powder compacts consolidated at 550 °C, as shown in Fig. 9a and b.

Fig. 9c and d display micrographs of the cross-section beneath the fracture surfaces of the tensile specimens, showing several cleavage cracks in the Si grains. These cleavage cracks are nucleation sites of the fracture. Since the Si grains are both hard and brittle, they are the first to crack as tensile stress increases, generating the cleavage planes shown in Fig. 9a and b.

4. Discussion

4.1. Characteristics of the powders in a semi-solid state

In thixocasting, a semi-solid metal forming process, the formability of a metal depends strongly on its thixotropic characteristics, including liquid content and microstructure.

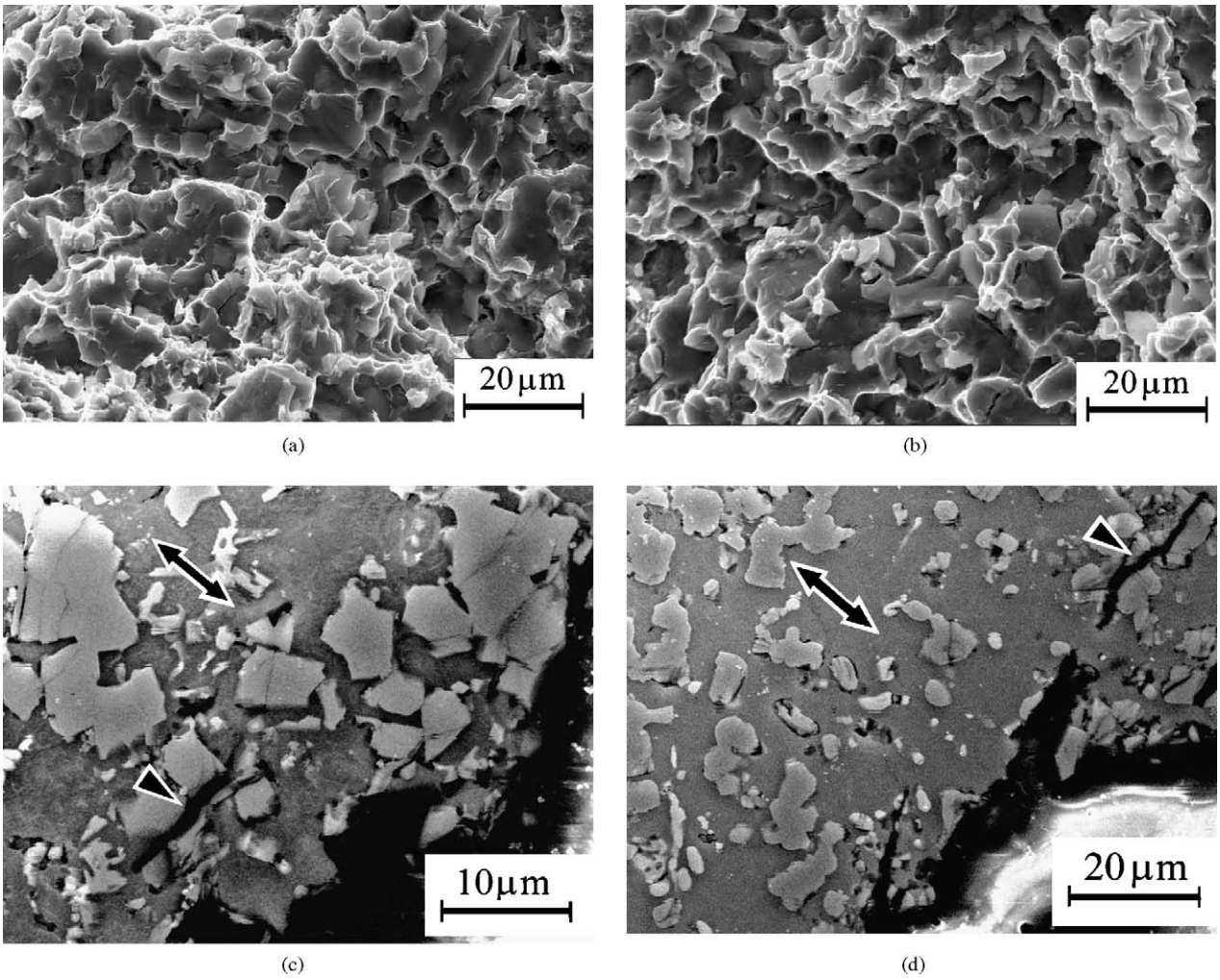

Fig. 9. Tensile fractographs of the powder-thixocast specimens in (a) as-cast and (b) T6-treated state. Cross-section micrographs of these specimens beneath the tensile fracture surfaces are shown in (c) for as-thixocast and (d) for T6-treated specimens. (↔) Indicated the tensile direction. The thixocast specimens were machined from the "plate" sections and fabricated using powders of size in 120–300 μm and compacts consolidated at 550 °C.

Besides the major constituents of 25 wt.% Si and 2.5 wt.% Cu, the powders used here also contain other minor elements such as 1.0 wt.% Mg, 0.47 wt.% Mn and 0.16 wt.% Fe, as listed in Table 1. Since the solubility of Mg in α-Al is as high as 17.1% at 450 °C, the 1 wt.% Mg could be totally dissolved in α-Al grains in as-atomized powders. Thus the 1 wt.% Mg would not affect the liquid fraction of the powders heated from solid state into a semi-solid state. The proportions of other minor elements of Mn and Fe in the powder were too small to influence the liquid content. Consequently, a ternary Al–Si–Cu phase diagram [10], Fig. 10, was used here to determine the liquid content and describe the microstructural evolution of the powders in the semi-solid state.

Fig. 10 presents an isothermal section of an Al–Si–Cu ternary phase diagram at 560 °C [10]. Point "E" is the ternary eutectic point of α-Al, $CuAl_2$ and Si, and is the lowest point of the liquid surface in the phase diagram. At Point "E", aluminum alloy contains 26.7 wt.% Cu and 5.2 wt.% Si, and melts at 525 °C [13,15]. In Fig. 2, an endothermic peak occurred with on-set temperature at 530 °C. Since this on-set temperature is close to the ternary eutectic point, we suggest that the formation of the melt starts with the ternary eutectic phases of α-Al, $CuAl_2$ and Si when the powder is heated to 530 °C.

Point "B" in Fig. 10 is the point of intersection between the isothermal planes at 560 °C and the eutectic valley. Point "P" represents the compositions of the powder used. Point "A" is the point of intersection of the line extended from Point "B" through "P" with the Al/Si side of the three-phase region. Using the lever rule, the liquid fraction at 560 °C can be approximated by AP/AB, at around 15 wt.%. This small amount of liquid may provide the fluidity required to deform the powders during powder-thixocasting.

In a binary Al–Si alloy, solid α-Al, Si grains and liquid melt cannot coexist, since the α-Al melts completely at a eutectic temperature of 577 °C. By adding some Cu to the hypereutectic Al–Si alloy, P.J. Ward [11] found that solid α-Al could be stabilized to coexist with Si grains and liquid

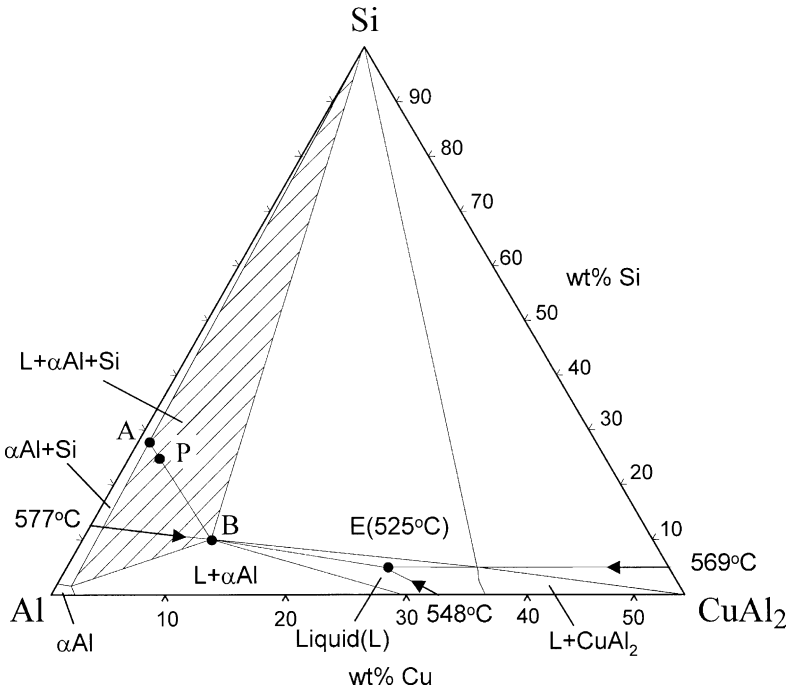

Fig. 10. The Al–Si–Cu isothermal phase diagram at 560 °C, depicted as that proposed by Ward [10,11]. Hatched zone shows three phases region, i.e. α-Al, Si and liquid. The compositions of the powder used are about 25 wt.% Si and 2.5 wt.% Cu, which is shown at Point "P" in this phase diagram. Dashed line A-P-B shows how equilibrium liquid contents are found using the level rule.

melt, as revealed in Fig. 10. However, α-Al was stabilized only in the early stage of melting to a semi-solid. In this work, stabilization occurred between 530 and 565 °C, as revealed in Fig. 2. On further heating of the powders above 565 °C, binary eutectic phases of α-Al and Si in the powders began to melt, α-Al + Si → Liquid [13]. This reaction quickly depletes the solid α-Al phase in the thixo-forming microstructured slurry, and finally solid Si grains remain suspended in the liquid melt. On further heating to 750 °C, the primary Si grains dissolve completely in the melt.

Fig. 2 also includes a small exothermic peak at 500 °C, during cooling. However, no corresponding endothermic peak appears at 500 °C during heating. This is because of the slow solidification of the powder during cooling stage in DTA testing, causing the reaction occurred, liquid → $Al + CuAl_2 + CuMgAl_2 + Mg_2Si$ [13]. However, the missing DTA peak at 500 °C during heating may be due to the super-saturation of Mg in rapidly solidified powders.

4.2. Kinetics of Si grain growth in semi-solid state

The kinetics of Si grain growth in the semi-solid state must be determined for thixocasting hypereutectic Al–Si alloys with fine Si grains. Table 3 shows that the Si grains ripened apparently when the powders were isothermally heat-treated at temperatures ranging from 540 to 600 °C. The driving force of Si grain growth is a decrease in the interfacial energy, due to a reduction in both the amount and the curvature of the Si grain-matrix interface. The classical Lifshittz Slyozov Wanger (LSW) theory [16–18] was applied here to analyze the grain growth behavior. For sparsely distributed spherical grains in a matrix under diffusion-controlled growth, the classical LSW theory predicts that the ripening process will yield a steady-state distribution of grain sizes and will cause the mean grain diameters (d) to increase with time (t) as [19,20]:

$$d^3 - d_0^3 = \frac{32Kt}{9} \quad (1)$$

where d_0 is the initial mean grain diameter, K is a rate (kinetic) constant given as follows:

$$K = \frac{2DCV_m\gamma}{RT} \quad (2)$$

where D is the diffusivity of the grain element through the matrix, C is the concentration of the grain element in the matrix, V_m is the molar volume of the grain, γ is the grain-matrix surface energy, R is gas constant, and T is the absolute temperature. Fig. 11 illustrates the Si grain size variations with isothermal heat-treatment time intervals and temperatures. The experimental values of Si grain sizes were plotted with discrete points and these points were line fitted using Eq. (1). The grain growth behaviors are consistent with the calculation using Eq. (1). The grain growth rate constants (K) at various isothermal heat-treatment temperatures can be determined from the gradients in Fig. 11. Since the diffusion involved in Si grain growth is thermally activated, the calculated rate constants (K) should depend exponentially on

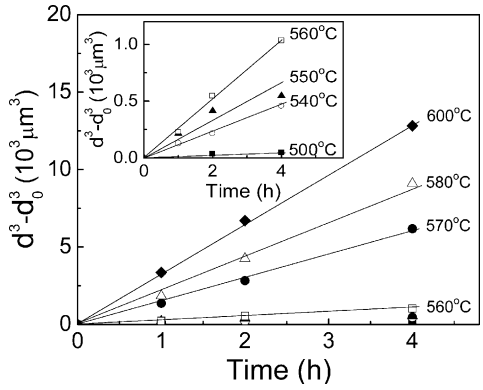

Fig. 11. Evolution of the average Si grain sizes (d) in the Al–25Si–2.5Cu–1Mg–0.5Mn powders (in size of 120–300 μm) as a function of isothermal heat-treatment temperatures and time intervals. d_0 is the average Si grain sizes in the as-atomized powders. The experimental values of Si grain sizes were plotted with discrete points and these points were line fitted according to the LSW theory. The inset shows the magnified graph for the temperature ranged from 500 to 560 °C.

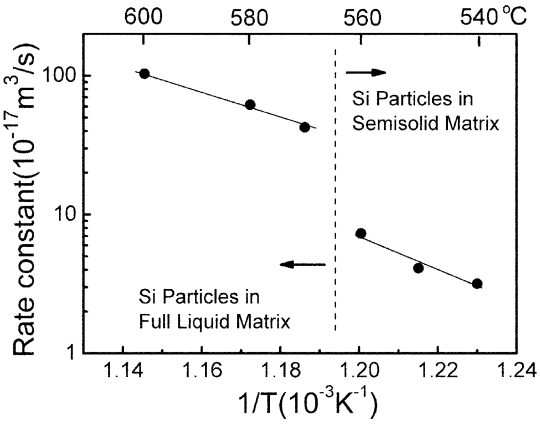

Fig. 12. Rate constants (kinetic) of Si grain growth versus the inverse of isothermal heat-treatment temperatures. Rate constants were obtained from linear dependence of the slope in plot Fig. 11.

temperature; that is, they should be proportional to exp($-Q/RT$), where Q is the activation energy. The value of Q can be obtained from the plot of the logarithm of the rate constant (K) against $1/T$, as shown in Fig. 12. Fig. 12 clearly shows that the rate constants in the semi-solid state fall into two distinct ranges. The rate constants at temperature below 565 °C are around one order of magnitude lower than those at a temperature above 565 °C. The calculated Q was 229 kJ/mol at a temperature below 565 °C and 174 kJ/mol above 565 °C. In this case, increasing the isothermal heat-treatment temperature also increased the liquid content in the matrix. Hence, the calculated activation energies did not closely correspond to the activation energy of diffusion of Si in an Al matrix at 500 °C, 126–138 kJ/mol [17].

Fig. 13 schematically depicts that the matrix of Si grains is in the semi-solid state from 540 to 565 °C and in the liquid state above 565 °C. Considering the thixocasting temperature used in this work, Si grain growth occurs by the transport of solute through the matrix. Eq. (2) shows that K is proportional to both diffusivity (D) and solubility (C). For a binary Al–Si alloy, the Si solubility in the liquid melt at 577 °C is 12.5 wt.%, which is much higher than that in α-Al solid, 1.65 wt.%. Furthermore, the Si diffusion coefficient in liquid Al melt is much higher than that in the solid Al matrix. For example, the Si diffusion coefficient in the solid Al matrix at 497 °C is only 1.6–2.2 × 10^{-9} cm^2/s [21], while that of Si grains in Al melt at 700 °C is only 81 × 10^{-5} cm^2/s [22]. Accordingly, Si grain ripened more quickly in the liquid matrix than in the semi-solid matrix, since both the diffusivity (D) and the solubility (C) of the Si in liquid Al is much higher than in solid Al. The addition of Cu in hypereutectic Al–Si alloy effectively stabilized solid α-Al in semi-solid state. This addition of Cu is considered to be the critical part for the novel process presented herein, for fabricating a hypereutectic Al–Si–Cu alloy with fine and evenly distributed primary Si grains.

4.3. Effects of detrimental interfaces on strength of powder-thixocast specimens

In conventional powder forging or extrusion, plastic deformation is used to consolidate prealloyed powders or powder mixtures. The deformation may close the inter-granular pores and disrupt the oxides to facilitate welding of the

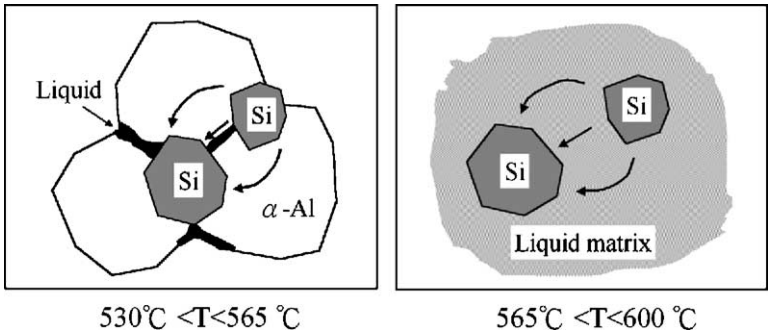

Fig. 13. Schematic diagrams of diffusion paths for Si grain growth process, showing that Si is transported through the Al alloy matrix, which is in semi-solid state at 530–565 °C, and in the liquid state at 565–600 °C.

powders [3]. Increasing the plastic deformation of the powder compacts has been demonstrated to increase the mechanical strength of the consolidated specimens [4,5]. In this study, a powder-thixocast mold with an extruding gate and runner, as depicted in Fig. 1d, were designed to use this consolidation mechanism. During powder-thixocasting, the semi-solid compact materials were first forged from a diameter of 76 mm to a diameter of 84 mm to fill the mold "biscuit" cavity. The materials were then extruded into the "runner" cavity in a process like forward extrusion, with a ratio of 7.84 and 90° angular extrusion. Finally, the materials were extruded to "plate" cavity from a thickness of 20–6 mm. Accordingly, the as-thixocast specimens in the "plate" sections clearly undergo the most deformation, and should have the highest tensile strength. Table 6 supports the prediction of the highest strength of the "plate" section. Consequently, this paper proposes that the mechanism for consolidating powder by plastic deformation can also be adapted to the powder-thixocasting process presented here.

Table 6 also shows that the thixocast specimens fabricated with compacts consolidated at 550 °C are stronger than those with compacts consolidated at 500 °C. Inter-granular pores and oxides were considered to explain this difference. Since the difference between the relative densities of these two thixocast specimens is small, as shown in Table 5, the strength difference is associated primarily with the interfacial oxides. Fig. 5a shows that the powder compacts consolidated at 500 °C have many inter-granular pores, resulting in poor bonding between individual powder particles. This weak bonding causes the deformation of the powder compacts by rotation or sliding of the individual powder particles during thixocasting. This rotation or sliding does not easily rupture the surface oxides on the powders. Fig. 8 shows a deep spherical cavity in the tensile fractographs, which is the evidence of the de-bonding of complete powder particles due to surface oxide. However, the powder compacts consolidated at 550 °C have fewer inter-granular pores than those consolidated at 500 °C, as shown in Fig. 5a and b. The individual powder particles can be deformed to rupture the oxides during the thixocasting of the compacts consolidated at 550 °C, increasing their strength.

Table 6 also shows that the thixocast specimens with smaller powders exhibit somewhat worse mechanical characteristics, which in fact follows from the larger specific surface areas and oxide films of smaller powders.

4.4. Feasibility of metal net-shape forming by powder-thixocasting

Nondendritic microstructures, or so-called thixotropic microstructures [23,24], are required to enable the feedstock to exhibit good formability during thixocasting. Since gas-atomized powders have nondendritic fine microstructures, powder compacts must have thixotropic microstructures. However, two other issues must be considered when fabricating powder-thixocasting specimens with integrity and fine microstructures. One issue concerns the oxide films and the inter-granular pores in the powder compacts, which may drastically reduce the strength of thixocast specimens. The other issue is microstructural coarsening during thixocasting, since the processing temperatures are very high and the powders partially melt.

In this work, the powder compacts were quickly heated by induction coils to a semi-solid state in less than 200 s. The short heating time can minimize the oxidation, even though the powder was heated in air. Additionally, as described above, plastic deformation during powder-thixocasting can eliminate the detrimental oxides and pores from the powder compacts. Furthermore, maintaining the processing temperature between 540 and 560 °C can prevent the Si grains from coarsening quickly. Table 6 indicates that the optimum strength of the as-thixocast specimens is 224.7 MPa and that of the T6 specimens is 304 MPa. However, the strength of hypereutectic Al–Si alloys fabricated by conventional powder forging can reach around 400 MPa [3]. The Si grains in thixocast specimens tend to aggregate near the α-Al grain boundary, as shown in Fig. 6. The cracks in the aggregated Si grains rapidly coalesce, as shown in Fig. 7c and d, which increase the velocity of crack propagation. The agglomerated Si grains in the specimens are believed to cause brittleness of these alloys, whose ductility is usually below 0.2%. Accordingly, the strength of the powder-thixocast specimens is lower than that obtained by powder forging. However, the results on strength presented here closely correspond to those of P.J. Ward [10], who thixocast the hypereutectic Al–Si–Cu alloys using spray-forming billets, also yielding aggregated Si grains. From the above descriptions, we therefore suggest that the powder-thixocasting process presented herein can feasibly and costly fabricate the hypereutectic Al–Si–Cu alloys in a net-shape with fine Si grains and moderate strength. The reason behind the powder thixocast Al–Si alloys having lower strength than those produced by powder forging is not only the tendency of aggregation and coarsening of Si grains in the former case, but also the additional strain hardening effects in the latter case. Nevertheless, powder-thixocasting offers an alternative to powder forging when a complex part of the hypereutectic Al–Si alloys is fabricated in net-shape forming.

Powder-thixocasting is a highly promising means of combining pressure-assisted consolidation in conventional powder metallurgy (PM) with newly developed semi-solid casting. This new method is believed to be able to carry out net-shape forming of various materials, except the hypereutectic Al–Si alloys, including metal matrix composites and metal alloys with precipitates stabilized at high temperature.

5. Conclusions

This paper studied a new process for fabrication of hypereutectic Al–Si alloys by thixocasting of densified powder compacts. The new process was demonstrated as a

feasible method for net-shape forming of the hypereutectic Al–25Si–2.5Cu–1Mg–0.5Mn alloys that have microstructures of integrity and evenly distributed Si grains.

Some conclusions can be drawn about the success of this process. By elemental addition of 2.5 wt.% Cu into the hypereutectic Al–Si alloy, α-Al grains could be stabilized to coexist with Si grains and melt in the powders. About 15 wt.% melt was formed in the powder compacts when the compacts were heated to 560 °C. The melt wet the solid α-Al and Si grains, thus the compacts could be deformed easily during thixocasting in semi-solid state. However, the stabilized α-Al grains would melt completely when the powder compacts were heated above about 565 °C. Thus the Si grains became suspended in the melt leading to extreme Si grains growth. Two distinct ranges of Si grain growth were found in semi-solid state of the powders. According to the LSW theory, the activation energies of Si grain growth were calculated to be 174 kJ/mol at temperatures above 565 °C and 229 kJ/mol below 565 °C. The rate constants of Si grain growth at temperatures above 565 °C are around one order of magnitude than those at temperatures below 565 °C. Therefore, heating the powder compacts to a temperature between 540 and 560 °C ensured adequate fluidity of the compacts and prevented the Si grains from coarsening rapidly during thixocasting. The tensile strengths of the thixocast specimens are strongly dependent on the elimination of interfacial oxide layers on the powders. Using large-sized powders, i.e. 120–300 μm, can decrease the quantity of powder surface oxides and raise the strength of thixocast specimens. In this study, the strength values of the as-thixocast and T6 specimens are 225 and 304 MPa, respectively, which are close to those thixocast using feedstock made by spray forming followed by extrusion. In powder-thixocasting presented here, the powder compacts could be deformed severely during thixocasting by adequate mold gating design. The severe plastic deformation of the powder compacts during thixocasting could effectively eliminate the detrimental interfacial oxides, yielding thixocast specimens with favorable strength characteristics.

Acknowledgements

The authors would like to thank the National Science Council of the Republic of China for financially supporting this research under Contract No. NSC 91-2216-E-009-022.

References

[1] J.E. Gruzleski, B.M. Closset, The Treatment of Liquid Aluminum-Silicon Alloys, AFS, Des Plaines, Illinos, 1990, pp. 107–126.
[2] J.E. Hatch, Aluminum: Properties and Physical Metallurgy, ASM, Metals Park, Ohio, 1984, pp. 346–347.
[3] K. Akechi, US Patent No. 4,838,936 (June 1989).
[4] H. So, W.C. Li, H.K. Hsieh, J. Mater. Process. Technol. 114 (2001) 18.
[5] J.W. Yeh, S.Y. Yuan, C.H. Peng, Mater. Sci. Eng. A252 (1998) 212.
[6] G. Krumpholz, PMI 24 (5) (1992) 303.
[7] D.B. Spencer, R. Mehrabian, M.C. Flemings, Metall. Trans. 3 (1972) 1925.
[8] D.H. Kirwood, Int. Mater. Rev. 39 (5) (1994) 173.
[9] M.C. Flemings, Metall. Trans. A 22A (1991) 957.
[10] P.J. Ward, H.V. Atkinson, P.R.G. Anderson, L.G. Elias, B. Gracia, L. Kahlen, J.-M. Rodriguez-Ibabe, Acta Mater. 44 (5) (1996) 1717.
[11] P.J. Ward, H.V. Atkinson, D.H. Kirkwood, C.M. Sellars, in: S.B. Brown, M.C. Flemings (Eds.), Proceedings of the Conference on Processing of Semi-Solid Alloys and Composites, TMS, Massachusetts, 1992, pp. 440–446.
[12] C.M. Chen, C.C. Yang,C.G.Chao, in:Y. Tsutsui, M. Kiuchi, K. Ichikawa (Ed.), Proceedings of the 7th International Conference on Semi-Solid Processing of Alloys and Composites, Tsukuba, Japan, 2002, pp. 759–764.
[13] L.F. Mondolfo, Aluminum Alloys: Structure and Properties, Butter-Worths, London, Boston, 1976, p. 645.
[14] L. Bäckerud, G. Chai, J. Tamminen, Solidification Characteristics of Aluminum Alloys, vol. 2, Foundry Alloys, AFS/SKANALUMINUM: Des Plaines, Illinos, 1990, pp. 211–216.
[15] J.E. Hatch, Aluminum: Properties and Physical Metallurgy, ASM, Metals Park, Ohio, 1984, p. 49.
[16] I.M. Lifshittz, V.V. Slyozov, J. Phys. Chem. Solids 19 (1961) 35.
[17] C. Wanger, Z. Elektrochem. 65 (1961) 581.
[18] G.W. Greenwood, Acta Metall. 4 (1956) 243.
[19] Randall M. German, Liquid Phase Sintering, Plenum Press, New York, London, 1985, pp. 127–155.
[20] J.W. Martin, R.D. Doherty, Stability of Microstructure in Metallic Systems, Cambridge University Press, New York, NY, 1976, pp. 154–243.
[21] L.F. Mondolfo, Aluminum Alloys: Structure and Properties, Butter-Worths, London, Boston, 1976, p. 28
[22] Bruce Chalmers, Physical Metallurgy, Wiley, New York, 1962, p. 384.
[23] W.R. Loue, M. Suery, Mater. Sci. Eng. A203 (1995) 1.
[24] K. Xia, G. Tausig, Mater. Sci. Eng. A246 (1998) 1.